Cerebral Cortex February 2011;21:374-384
doi:10.1093/cercor/bhq105
Advance Access publication June 7, 2010

Neural Origin of Spontaneous Hemodynamic Fluctuations in Rats under Burst–Suppression Anesthesia Condition

Xiao Liu[1,2], Xiao-Hong Zhu[1], Yi Zhang[1] and Wei Chen[1,2]

[1]Center for Magnetic Resonance Research, Department of Radiology and [2]Department of Biomedical Engineering, University of Minnesota, Minneapolis, MN, USA

Address correspondence to Wei Chen, PhD, Center for Magnetic Resonance Research, Department of Radiology, University of Minnesota, 2021 6th Street SE, Minneapolis, MN 55455, USA. Email: wei@cmrr.umn.edu.

Spontaneous hemodynamic signals fluctuate coherently within many resting-brain functional networks not only in awake humans and lightly anesthetized primates but also in animals under deep anesthesia characterized by burst–suppression electroencephalogram (EEG) activity and unconsciousness. To understand the neural origin of spontaneous hemodynamic fluctuations under such a deep anesthesia state, epidural EEG and cerebral blood flow (CBF) were simultaneously recorded from the bilateral somatosensory cortical regions of rats with isoflurane-induced burst–suppression EEG activity. Strong neurovascular coupling was observed between spontaneous EEG "bursts" and CBF "bumps," both of which were also highly synchronized across the 2 hemispheres. Functional magnetic resonance imaging (fMRI) was used to image spontaneous blood oxygen level–dependent (BOLD) signals under the same anesthesia conditions and showed similar BOLD "bumps" and dependence on anesthesia depth as the CBF signals. The spatiotemporal BOLD correlations indicate a strong but less-specific coherent network covering a wide range of cortical regions. The overall findings reveal that the spontaneous CBF/BOLD fluctuations under unconscious burst–suppression anesthesia conditions originate mainly from underlying neural activity. They provide insights into the neurophysiological basis for the use of BOLD- and CBF-based fMRI signals for noninvasively imaging spontaneous and synchronous brain activity under various brain states.

Keywords: burst–suppression anesthesia, functional MRI, hemodynamic fluctuation, neurovascular coupling, spontaneous brain activity

Introduction

Recent findings from resting-state functional magnetic resonance imaging (fMRI) studies have increased the interest in imaging and studying spontaneous brain activity under a resting state in the absence of brain stimulation or task performance. These studies indicate that the blood oxygenation level–dependent (BOLD) (Ogawa et al. 1990, 1992; Bandettini et al. 1992; Kwong et al. 1992) signals acquired by fMRI in a resting brain are characterized by slow (<0.1 Hz) and coherent fluctuations within a variety of specific brain networks related to, for example, the motor, visual, auditory, thalamus, hippocampus, language, and default-mode systems (Biswal et al. 1995; Lowe et al. 1998; Cordes et al. 2000; Stein et al. 2000; Hampson et al. 2002; Greicius et al. 2003; Fox and Raichle 2007; Fair et al. 2008). The spatiotemporal correlations of spontaneous BOLD fluctuations have been hypothesized to reflect the "functional connectivity" (Biswal et al. 1995) between the different brain regions and imply many resting-state functional networks (Fox and Raichle 2007; Mantini et al. 2007).

Despite their great potential and importance, the neurophysiology underlying coherent BOLD fluctuations in a resting brain is not fully understood; in particular, it is still not clear whether they have a neural origin, vascular origin, or both (Lund 2001). Even though most evidence suggests a possible neural origin, there is still debate over whether the resting-state BOLD signals simply reflect the fluctuations of unconstrained and consciously directed mental activity or coherent networks with significant functional meaning (Morcom and Fletcher 2007). This argument was partially resolved when the resting-state fMRI research was recently extended from conscious human subjects to anesthetized unconscious nonhuman primates. Based on the correlations of spontaneous BOLD signals acquired from isoflurane-anesthetized primates, 4 distinct spontaneous coherent networks were identified, even under deep anesthesia (using 1.25% isoflurane) showing burst–suppression electroencephalogram (EEG) activity (Vincent et al. 2007), which is a clinical indicator of unconsciousness. This finding suggests that spontaneous BOLD fluctuations and coherent networks implied by the spatiotemporal BOLD correlations persist even in an unconscious brain without normal perceptions and behaviors. It was therefore hypothesized that coherent BOLD fluctuations may represent a fundamental and intrinsic property of functional brain organization (Vincent et al. 2007). It is, therefore, of great importance to understand the neurophysiological basis of spontaneous hemodynamic fluctuations under the unconscious brain state induced by deep anesthesia. The present study aimed to quantitatively investigate the neurovascular coupling relation between spontaneous hemodynamic fluctuations and neuronal activity in the rat brain under deep anesthesia characterized by burst–suppression EEG activity, and thus to understand the underlying mechanisms of spontaneous hemodynamic fluctuations in the brain under an unconscious state.

This study consisted of 2 experiments. In the first experiment, spontaneous cerebral blood flow (CBF) signals were measured simultaneously with epidural EEG signals from the bilateral somatosensory cortices of rats with isoflurane-induced burst–suppression anesthesia. The neurovascular coupling was examined and quantified using the temporal correlation between the CBF and EEG signals. In the second experiment, fMRI was used to image spontaneous BOLD signals from another group of rats under the same anesthesia conditions as used for the simultaneous EEG-CBF measurements. Spatiotemporal correlations of BOLD fluctuations were then examined and used to generate correlation maps. For both experiments, data acquisition were repeated under 3 isoflurane

levels of ~1.8%, ~2%, and ~2.2% (defined as ISO 1.8, ISO 2.0, and ISO 2.2 anesthesia conditions in this study), and the correlation strength and fluctuation magnitude of spontaneous BOLD/CBF signals were quantified for each anesthesia level. By quantitatively comparing the temporal and spatial characteristics of hemodynamic signals (CBF and BOLD) and their dependence on anesthesia level, we linked the results of both experiments and drew conclusions.

Materials and Methods

Simultaneous EEG-CBF Experiments

Six male Sprague–Dawley rats (289–389 g body weight) were anesthetized with ~2% isoflurane in a mixture of O_2 and N_2O gases with a 2:3 volume ratio. The femoral artery and vein were catheterized for physiological monitoring and/or blood gas sampling. The animal respiratory rate and volume were controlled mechanically using a ventilation machine. During the experiments, the mean arterial pressure (MAP), inspired/expired O_2, CO_2, N_2O, body temperature, and heart rate were continuously monitored and recorded. The MAP and heart rate results are summarized in Table 1, and no substantial changes were found in any of the 3 anesthesia conditions. Arterial blood gas was sampled every 1–2 h, and all parameters (pO_2, pCO_2, pH, and plasma glucose level) were maintained within normal physiological limits.

One EEG electrode was grounded on the animal's nose, and the other 2 EEG electrodes were inserted symmetrically, through 2 small holes in the skull, into the cortical regions of S1FL (the primary somatosensory cortex in rat forelimb) (~1.5 mm deep from the surface of the skull, ~1.5 mm posterior to the bregma, and ~3 mm lateral to the brain midline) in the 2 hemispheres. The EEG signals were sampled at 1 kHz using commercially available EEG equipment (Grass-Telefactor) and then filtered with a band-pass filter (0.1–30 Hz). A dual-channel laser doppler flowmetry (LDF) instrument (OxyLab LDF/OxyFlo, Oxford Optronix) was used to measure regional relative CBF changes simultaneously with the EEG measurement. Two LDF probes were inserted into the somatosensory cortices slightly under the EEG electrodes through the same skull holes. The CBF signals were acquired at a sampling rate of 10 Hz. The simultaneous CBF/EEG recordings were performed under 3 anesthesia conditions using 1.8%, 2.0%, and 2.2% isoflurane, respectively, and as well after the rats were sacrificed with a bolus injection of KCl solution. Animal surgical procedures and experimental protocols were approved by the Institutional Animal Care and Use Committee of the University of Minnesota.

MRI Experiments

Ten male Sprague–Dawley rats (288–381 g body weight) were used for MRI experiments. The animal preparations were identical to those for the simultaneous EEG-CBF recording experiments. The head position of the rat was fixed by a home-built head-holder with a mouth bar and ear bars for minimizing head motion. All MRI studies were performed on a 9.4-T horizontal magnet (Magnex Scientific) interfaced with a Varian INOVA console (Varian Inc.) using a proton radiofrequency surface coil. First, the multislice T_1-weighted anatomical images were acquired from different orientations to identify the rat somatosensory cortex and select appropriate image slice positions for acquiring fMRI data. Second, the gradient-echo echo-planar image (GE-EPI) (Mansfield 1977) was used to acquire 5 consecutive coronal fMRI slices (field of view = 3.2 × 3.2 cm^2; repetition time/echo time = 612/16.5 ms; 64 × 64 image matrix size; 1-mm slice thickness) covering the rat somatosensory cortex (–4.3 to 0.7 mm from the bregma) by referring to the stereotaxic rat brain atlas (Paxinos and Watson 1998). All fMRI BOLD signals were acquired when the rats were in complete darkness. The fMRI measurements were conducted for 3 rats under the ISO 1.8 and ISO 2.0 conditions; for 3 different rats under the ISO 1.8, ISO 2.0, and ISO 2.2 conditions; and for the remaining 4 rats under the ISO 1.8, ISO 2.0, and ISO 2.2 conditions, as well as approximately 5 min after being sacrificed.

The fMRI acquisition was repeated 2–5 times under each condition, and each run included 500 GE-EPI volumes (~306 s).

Table 1
MAP and heart rate under varied anesthesia levels

Anesthesia conditions	Mean arterial pressure (mean ± SD)	Heart rate (mean ± SD)
ISO 1.8 (n = 16)	98.2 ± 8.3	359 ± 21
ISO 2.0 (n = 16)	97.6 ± 6.8	360 ± 23
ISO 2.2 (n = 13)	93.0 ± 10.5	358 ± 24

Data Processing

The simultaneously recorded EEG and CBF time courses were first divided into 300-s segments, and the segment duration was close to the total imaging time of 1 fMRI run. The EEG data were downsampled to 100 Hz by averaging every 10 data points to retain the signal-to-noise ratio (SNR). The amplitude of EEG signals was extracted by Hilbert transform and then convolved with a hemodynamic response function (HRF), which was determined in anesthetized rats in a previous study (Martin et al. 2006), to generate the EEG-predicted CBF time courses that were further downsampled to 10 Hz to match the temporal resolution of the experimentally measured CBF time courses.

The experimentally measured CBF signals were band-pass filtered (0.005–0.1 Hz) in the Fourier domain to remove the baseline drift and high-frequency noise.

For each fMRI run, all GE-EPI images were first spatially filtered with a Gaussian kernel (full width at half maximum = ~1 mm) to increase SNR, and the first 20 image volumes were discarded to avoid transient BOLD signals at the initial image acquisition stage. The time course of each image pixel was normalized by its mean and then band-pass filtered (0.005–0.1 Hz) to remove the DC component, linear drift, and high-frequency noise. The standard deviations (SDs) of BOLD time courses were then calculated to generate a SD map for each fMRI run. A 2 × 2–pixel region located in the right S1FL region was selected as the reference region, which was close to the locations of the EEG electrodes and LDF probes in the EEG-CBF measurements. The BOLD time courses of all image pixels were then crosscorrelated (Pearson's correlation) with the reference time course extracted from the S1FL reference region to generate a correlation coefficient (CC) map for each fMRI run. In addition, 2 regions of interest (ROIs) were selected from the cortical regions, mainly covering the left and right S1FL according to the anatomical images, for statistical analysis.

Statistics

To quantify the strength of neurovascular (EEG-CBF) coupling, the temporal CCs between the EEG-predicted CBF and the experimentally measured CBF time courses were calculated as a function of temporal lags for each segment.

To quantify the interhemisphere correlation of the spontaneous CBF signals, CCs between the CBF signals measured from 2 brain hemispheres for each segment were calculated. To quantify the interhemisphere correlation of the spontaneous BOLD signals, the CCs of each CC map were averaged within the left S1FL ROI (contralateral to the S1FL reference region) to give an average CC for each fMRI run.

To quantify the fluctuation magnitude of spontaneous CBF signals, the SD of the normalized CBF signals was calculated for each segment. The SD was also calculated for EEG-predicted CBF signals (arbitrary units) and then normalized by the value observed under the ISO 1.8 anesthesia condition. To quantify the fluctuation magnitude of spontaneous BOLD signals, the SD maps of each fMRI run were averaged within the 2 S1FL ROIs defined previously.

To test whether the baseline levels of CBF and fMRI signals change at different anesthesia depths, the mean CBF and fMRI signals (averaged within the S1FL ROIs) were calculated for each segment (or run) acquired under the 3 anesthesia conditions; the results were then normalized by that of the ISO 1.8 anesthesia condition.

Finally, a linear mixed model taking the rats as the random variable and the isoflurane anesthesia level as the fixed variable was used to summarize the statistics from all rats and give the statistical inference. The statistical analyses were performed in R (R Development Core Team 2008) using the "nlme" package (Pinheiro et al. 2009). A P value of ≤ 0.01 was considered to be statistically significant.

Results

Temporal Correlations between Spontaneous EEG and CBF Changes

Figure 1 shows the EEG and CBF time courses measured in the bilateral S1FL regions from a representative rat under the 3 anesthesia conditions. The EEG signals measured under the ISO 1.8 and ISO 2.0 conditions exhibited a typical burst–suppression EEG pattern: quasiperiodical bursts of high-voltage slow wave (mainly <15 Hz) separated by suppression periods of a low-voltage flat EEG pattern lasting from a few seconds to a few minutes (Stern and Engel 2005; Kroeger and Amzica 2007). Interestingly, the distinct EEG "bursts" were always followed by corresponding triangular-shaped "bumps" in the CBF time courses simultaneously recorded in the same S1FL region. This observation is consistent with an early study (Golanov et al. 1994), qualitatively suggesting a close neurovascular coupling between the spontaneous EEG and CBF signal changes. When the anesthesia level was increased from ISO 1.8 (Fig. 1*A*) to ISO 2.0 (Fig. 1*B*), the appearance frequency of the spontaneous EEG bursts was largely reduced and the number of CBF bumps also decreased accordingly. Once anesthesia reached the deepest level of ISO 2.2, the EEG burst activity almost disappeared and only single spikes were occasionally observed; correspondingly, the CBF fluctuations were almost flat (Fig. 1*C*). The relation between the isoflurane concentration and the appearance frequency of EEG bursts is shown in Supplementary Figure S1.

The EEG-predicted CBF time courses (thick black traces in Fig. 1) were highly correlated to the experimentally measured CBF time courses (red traces in Fig. 1) under the different anesthesia conditions, and their CCs are plotted in Figure 2 as a function of temporal lags. The EEG-CBF coupling was very strong under the ISO 1.8 and ISO 2.0 anesthesia conditions with CCs of 0.61 ± 0.17 and 0.65 ± 0.20 (mean ± SD) at the zero lag, respectively. In contrast, the correlation was significantly reduced to 0.28 ± 0.21 under the ISO 2.2 condition and disappeared (0.02 ± 0.07, not statistically different from zero) when EEG activity became completely silent after the animal was sacrificed. These results indicate that a tight EEG-CBF correlation exists in the deeply anesthetized (but not dead) rat brain.

Besides the tight correlation between the EEG and CBF signals acquired from the same S1FL cortical region, both EEG and CBF signals themselves were also found to be strikingly synchronized across the 2 brain hemispheres, in particular, under the ISO 1.8 and ISO 2.0 conditions (Figs 1*A*,*B*). Such strong interhemisphere correlations suggest that both spontaneous neuronal activity and coupled CBF fluctuations are highly synchronized within somatosensory cortices under these 2 deeply anesthetized unconscious conditions.

Spatiotemporal Correlations of Spontaneous BOLD Fluctuations

Compared with the CBF signals recorded using the dual-channel LDF system, the fMRI BOLD signals have a larger coverage and can provide more information about the spatial distribution of spontaneous hemodynamic fluctuations. To obtain such information, correlation maps were generated by correlating

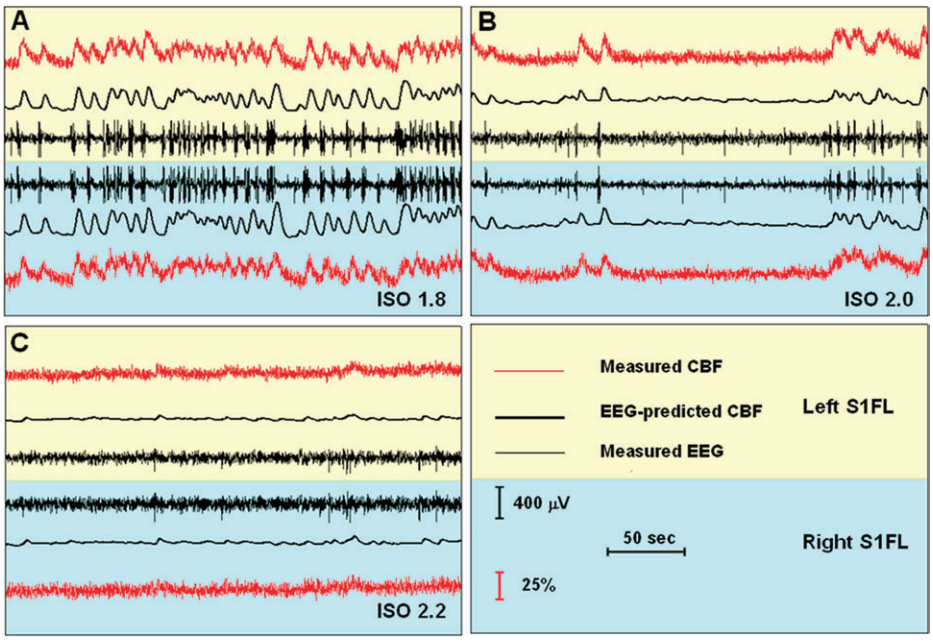

Figure 1. Spontaneous EEG and CBF signals simultaneously recorded from bilateral S1FL regions of a representative rat under varied anesthesia depths: (*A*) ISO 1.8: 1.8% isoflurane, (*B*) ISO 2.0: 2.0% isoflurane, and (*C*) ISO 2.2: 2.2% isoflurane. Each "burst" in the EEG time courses (thin black traces) was always followed by a triangular-shaped "bump" in the simultaneously recorded CBF signals (thin red traces, unfiltered). The EEG-predicted CBF time course (thick black traces), which is the convolution of the EEG amplitude and a HRF, was very similar to the measured CBF time course. Moreover, both the temporal EEG and CBF changes were highly synchronized between the left (light yellow background) and right (light blue background) hemispheric S1FL. The appearance frequency of spontaneous EEG "bursts" and CBF "bumps" decreased as anesthesia became deeper, and they almost disappeared under the deepest ISO 2.2 anesthesia condition.

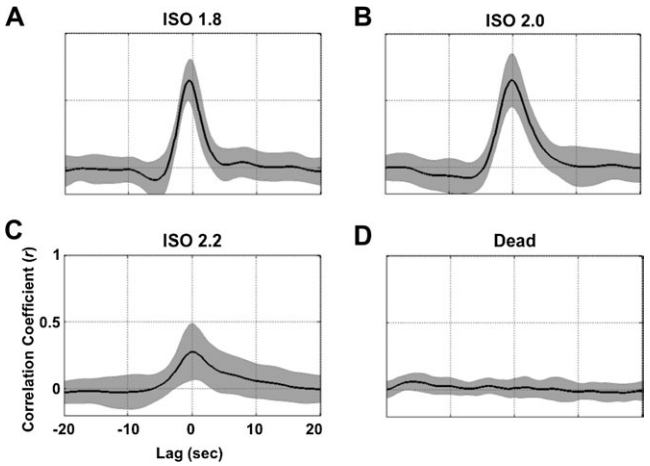

Figure 2. CCs between the EEG-predicated and measured CBF signals as a function of temporal lags under different anesthesia conditions. The black curves present crosscorrelation functions averaged over different segments from 6 rats, and the gray shadows represent regions within 2 SDs. Correlations were strong under (*A*) the ISO 1.8 and (*B*) ISO 2.0 anesthesia conditions, reduced significantly under (*C*) the ISO 2.2 anesthesia condition, and finally approached zero (*D*) after the rats were sacrificed.

spontaneous BOLD signals of all image pixels with that of a reference region (the blue cross in Fig. 3) located in the right S1FL (Paxinos and Watson 1998). The correlation maps from a representative rat (Rat 8) are shown in the left panel of Figure 3. Under the ISO 1.8 and ISO 2.0 conditions, the spontaneous BOLD fluctuations showed strong correlation over the majority of the cortical regions covered by the 5 acquired fMRI slices, which mainly included the brain regions of M1, M2, S1HL, S1FL, S1DZ, S1BF, and S2 (Paxinos and Watson 1998) associated with sensorimotor functions. In contrast, the correlations of spontaneous BOLD signals were much weaker at the ISO 2.2 anesthesia level. After the rats were sacrificed but with the air ventilation still running, only the reference region appeared in the correlation maps due to autocorrelation, and its correlation with other brain regions completely disappeared as illustrated in Figures 3 and 4. These results suggest that the physiological noise from periodic respiration had a negligible effect on the BOLD time courses measured in a live rat brain in this study.

To further understand the anesthesia-level-dependency of BOLD, for each anesthesia condition the BOLD signals were extracted from both the reference S1FL region (the blue cross in Fig. 3) and the contralateral S1FL region (the yellow cross in Fig. 3) and are plotted on the right side in Figure 3 (the right panel) next to their corresponding correlation maps. Interestingly, the BOLD signals acquired under the ISO 1.8 and ISO 2.0 conditions have triangular-shaped bumps, which highly resemble those CBF bumps observed in the first experiment (e.g., shown in Fig. 1). The BOLD bumps have a fast rising phase and a slow declining phase; they appear less frequently as the anesthesia level deepens and disappear under the ISO 2.2 anesthesia condition. Moreover, these bumps are highly synchronized between the bilateral S1FL regions and result in a strong BOLD correlation between those cortical regions. The correlation maps averaged over multiple fMRI runs are shown in Figure 4 for all 10 rats to demonstrate the excellent reproducibility and reliability of the fMRI BOLD measurements across individual rats. The reproducibility and reliability were further demonstrated in detail in the Supplementary Material (see Supplementary Figs S2 and S3).

Besides the cortical regions, the subcortical regions including some thalamic nuclei and the caudate putamen (CPu) also show correlations to the reference S1FL region, especially under the ISO 1.8 anesthesia condition, although to a lesser extent compared with corticocortical correlation. Figure 5 demonstrates the correlation maps measured from a single fMRI run from 2 rats showing the strongest cortical–subcortical correlations. From the posterior to anterior brain position, the correlated subcortical regions move from the thalamic nuclei, mainly including the posterior thalamic nucleus, ventral posterolateral thalamic nucleus, ventral posteromedial thalamic nucleus, and ventral anterior thalamic nucleus to the CPu accordingly. This observation is consistent with the anatomy of the rat brain (Paxinos and Watson 1998). Although the strength of such cortical–subcortical correlations varied across individual rats, the spatial correlation pattern was consistent among them.

Multimodal Comparison and Statistical Summary

To quantitatively illustrate the above observations, statistics for evaluating the coherence strength and fluctuation magnitude of spontaneous CBF and BOLD signals were calculated and are summarized according to anesthesia levels (Fig. 6). The fluctuation magnitudes of the experimentally measured CBF, the EEG-predicted CBF (Fig. 6*A*), and BOLD signal (Fig. 6*C*), which were quantified by the SD of normalized signals, decrease with very similar trends as the anesthesia depth increases. The similar dependences led to 2 excellent linear relations of fluctuation magnitudes under varied anesthesia conditions: one between the CBF and BOLD signals and the other between the EEG-predicted CBF and BOLD signals (Fig. 6*B*). These results suggest tight coupling among spontaneous BOLD, CBF, and EEG signals.

Although a significant difference in fluctuation magnitude was found between the ISO 1.8 and ISO 2.0 anesthesia conditions ($P = 2.98 \times 10^{-3}$ for CBF, $P = 5.37 \times 10^{-11}$ for EEG-predicted CBF, and $P = 4.03 \times 10^{-8}$ for BOLD), the coherence strength quantified by the interhemisphere CC did not differ significantly (Fig. 6*D*) between these 2 conditions ($P = 0.56$ for CBF and $P = 0.22$ for BOLD). However, it was significantly reduced under the ISO 2.2 condition ($P = 7.20 \times 10^{-7}$ for CBF and $P = 3.36 \times 10^{-18}$ for BOLD compared with ISO 1.8), and more drastically after the animals were sacrificed ($P = 8.53 \times 10^{-42}$ for BOLD compared with ISO 1.8).

Again, the coherence strength of the CBF and BOLD signals showed a very similar dependence on anesthesia level (Fig. 6*D*). All of these results confirm and support the observations based on the EEG and CBF time courses and functional BOLD correlation maps shown in Figures 1–4.

To further examine whether the anesthesia level could change the baseline level of CBF and fMRI signals (i.e., T_2^*-weighted GE-EPI signals), and thus influence the quantification of CBF and BOLD fluctuation magnitudes, the mean CBF and fMRI signals obtained under all conditions were normalized by those of the ISO 1.8 condition, and the results are summarized in Figure 6*E*. No statistically significant difference was found between the 3 anesthesia conditions (for CBF signal: $P = 0.07$ under ISO 2.0 and $P = 0.25$ under ISO 2.2; for fMRI signal: $P = 0.19$ under ISO 2.0 and $P = 0.65$ under ISO 2.2; compared with ISO 1.8 condition). After the animals were sacrificed, the baseline CBF approached zero and the baseline fMRI signal

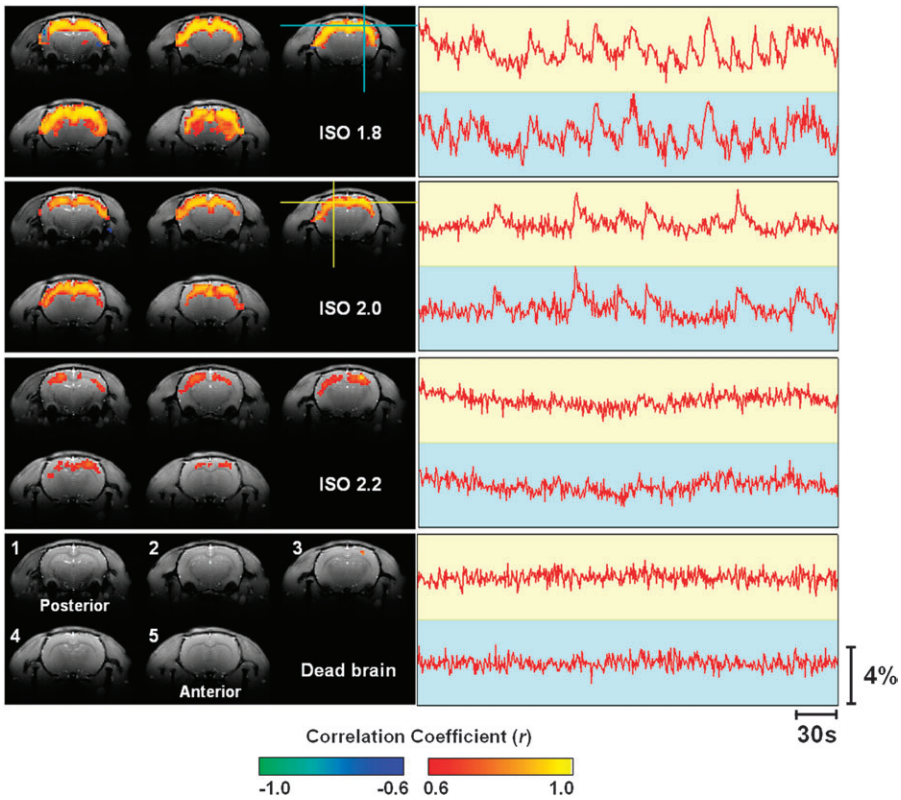

Figure 3. BOLD correlation maps and time courses measured under 3 anesthesia conditions from a representative rat brain (Rat 8). The reference region for the correlation maps was located at the right S1FL region. The 5 coronal fMRI slices (ordered from 1 to 5) were located −3.8, −2.8, −1.8, −0.8, and 0.2 mm from Bregma, respectively. The BOLD time courses were extracted from both the reference region (blue cross) and the contralateral S1FL region (yellow cross) without being filtered and plotted on backgrounds with the corresponding colors. Spontaneous "bumps" similar to those CBF bumps appeared frequently on the BOLD time courses acquired under the ISO 1.8 and ISO 2.0 anesthesia conditions. * The baseline fMRI signal acquired from the dead brain was smaller than the other 3 conditions (see Fig. 6*E*).

level decreased by 21.2% ($P = 1.76 \times 10^{-18}$), simply due to a large reduction in the brain blood oxygenation level.

Discussion

Neural Origin of Spontaneous Hemodynamic Fluctuations

In this study, tight neurovascular coupling was found between the colocalized EEG and CBF signals simultaneously recorded from the rat somatosensory cortex under burst–suppression anesthesia conditions. The spontaneous high-voltage bursts in EEG signals, which presumably result from the strong synchronization of neuronal activity from a large population of neurons, induce triangular-shaped CBF bumps with a few seconds of latency from the EEG bursts (Fig. 1). Increasing the anesthesia level can reduce the appearance frequency of EEG bursts and CBF bumps, which in turn can reduce the magnitude of spontaneous CBF fluctuations. Moreover, both the EEG bursts and CBF bumps are highly synchronized between 2 recording sites located in the bilateral S1FL regions in the 2 hemispheres.

The fMRI BOLD signals acquired under the same anesthesia conditions also show spontaneous bumps, which have a very similar shape to the CBF bumps (Figs 1 and 3). The similarity between spontaneous BOLD and CBF fluctuations is also evident from their strong synchronization over the large scale of 2 hemispheres and their similar dependence upon anesthesia depth. Quantification and comparison of the interhemisphere correlation strength and fluctuation magnitude of spontaneous CBF and BOLD signals provide statistical evidence to support the tight CBF-BOLD relation in a deeply anesthetized brain (Fig. 6). This finding is in line with the theory that BOLD contrast is usually dominated by CBF change (Ogawa et al. 1998).

The overall results of excellent EEG-CBF and CBF-BOLD correlations from the present study suggest that the spontaneous hemodynamic (CBF and BOLD) fluctuations observed under the burst–suppression anesthesia conditions are mainly induced by spontaneous high-voltage burst activity, and the synchronization of these spontaneous EEG bursts across a large population of neurons results in the strong correlation of hemodynamic fluctuations over different brain regions. This notion can probably be generalized to different species under similar burst–suppression anesthesia, for instance, isoflurane-anesthetized primates in which a number of coherent networks were identified based on the spatiotemporal correlations of spontaneous BOLD fluctuations (Vincent et al. 2007).

Previous studies have suggested that the spontaneous low-frequency hemodynamic fluctuations may have both neural and vascular origins (Hudetz et al. 1992; Biswal et al. 1997; Kannurpatti et al. 2008). In the present study, under the ISO 1.8 and ISO 2.0 anesthesia conditions, the high-voltage EEG bursts induced large bumps in the CBF (~25% peak-to-peak change, Fig. 1) and BOLD (~3% peak-to-peak change, Fig. 3)

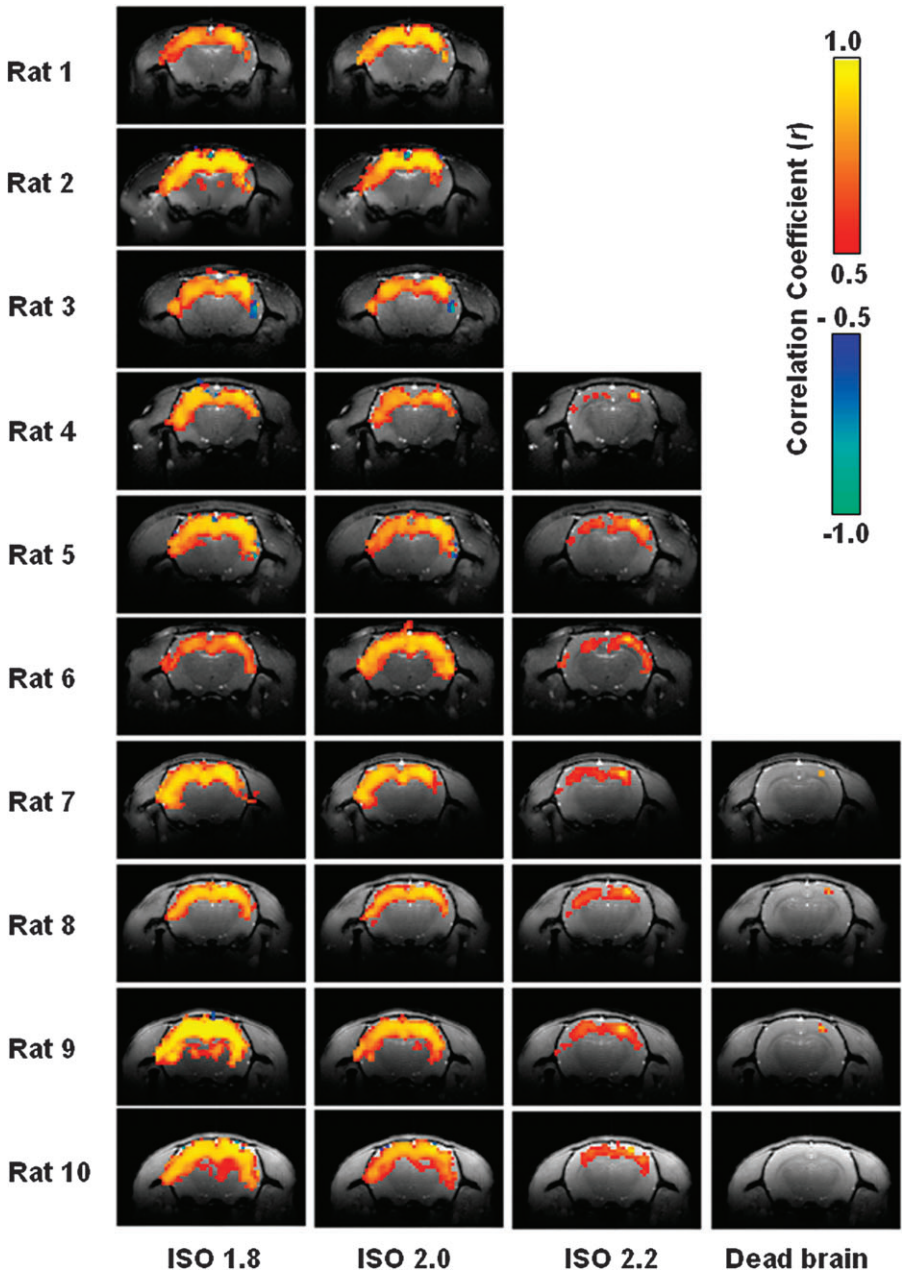

Figure 4. BOLD correlation maps measured under different anesthesia conditions from all individual rats studied. For each rat, the correlation maps present the results averaged from multiple fMRI runs acquired under the same condition.

signals with almost a one-to-one relation (Figs 1 and 3) and strikingly high coherence. Therefore, they are likely the major source leading to the spontaneous CBF and BOLD fluctuations observed under these conditions. However, when the anesthesia level is further increased to ISO 2.2 and EEG activity becomes much quieter (Fig. 1*C*), it is not clear whether or not other sources such as the vascular component could make substantial contributions since the neurovascular coupling becomes much weaker (Fig. 2*C*). This aspect deserves further investigation.

Previous animal studies (Hudetz et al. 1992; Kannurpatti et al. 2008) also showed that a significant reduction in MAP under certain severe conditions, such as exsanguination, can affect the autoregulation function of the vascular system and result in strong low-frequency fluctuations of CBF (Hudetz et al. 1992) and BOLD (Kannurpatti et al. 2008) signals. To avoid this complication, all the CBF and BOLD data acquired in the present study were obtained when physiological parameters including MAP and heart rate were stable and within a normal physiological range. There were no substantial MAP or heart rate variations among the 3 anesthesia conditions (Table 1). It is interesting to note that MAP was slightly higher under the relatively lighter anesthesia conditions (ISO 1.8 and ISO 2.0; Table 1) in which we observed stronger CBF/BOLD fluctuations and coherence. Therefore, the dependence of hemodynamic fluctuations on anesthesia depth found in the

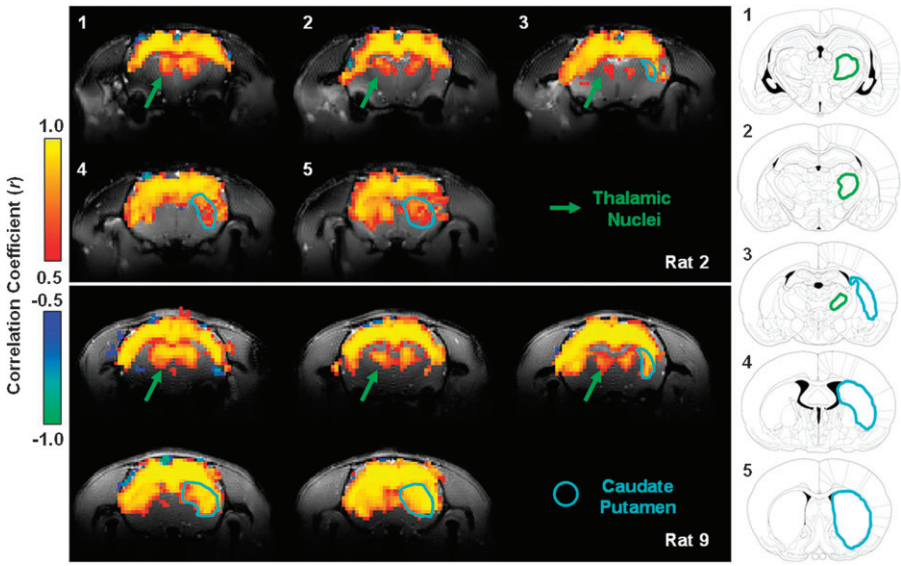

Figure 5. Demonstration showing the coherent BOLD fluctuations between the cortical and subcortical regions. Left panel: the correlation maps under the ISO 1.8 anesthesia condition based on single fMRI runs acquired from 2 rats (Rat 2 and Rat 9). The green arrows point out thalamic regions and the blue lines delineate the CPu. Right column (adopted from the rat brain atlas [Paxinos and Watson 1998]): the corresponding anatomical drawings for all fMRI slices. The regions delineated by the blue lines are belong to the CPu, and the areas outlined with green lines mainly cover several thalamic nuclei including the posterior thalamic nucleus, ventral posterolateral thalamic nucleus, ventral posteromedial thalamic nucleus, and ventral anterior thalamic nucleus.

present study cannot be attributed to the vascular autoregulation associated with MAP variation.

Neural Correlates of Spontaneous Hemodynamic Fluctuations

A number of studies have demonstrated or suggested the neural correlates of spontaneous hemodynamic fluctuations in different species under various brain states. Spontaneous BOLD signals in the occipital lobe of awake human subjects were found to be negatively correlated with α-band EEG activity from the same brain region (Goldman et al. 2002; Moosmann et al. 2003; Feige et al. 2005). In addition, the power fluctuation of δ-band EEG activity was suggested to contribute significantly to the spontaneous cerebral blood volume (CBV) fluctuations in α-chloralose–anesthetized rats (Lu et al. 2007), based on the finding of the similar interhemisphere correlation dependence of CBV and δ-band EEG on anesthesia level. It is also interesting to note that spontaneous BOLD fluctuations in lightly anesthetized primates were found to be correlated with γ-band local field potential activity, multiunit activity, and neuronal spiking rates (Shmuel and Leopold 2008), although this result is still under debate (Logothetis et al. 2009).

Compared with the studies reported in the literature, the neurovascular coupling observed under the burst–suppression anesthesia condition in the present study seems to be much stronger, probably due to the quasiperiodical alternation between high-voltage EEG bursts and low-voltage EEG suppression patterns. Furthermore, the time–frequency analysis from a previous electrophysiological study (Hudetz and Imas 2007) indicated that the relatively low-frequency band (9–12 Hz) activity dominates such spontaneous EEG bursts under burst–suppression anesthesia.

One possible explanation for the discrepancies in the way different types of spontaneous neural activities (e.g., γ-band LFP, δ-band, α-band EEG, and burst–suppression EEG activity) are correlated with spontaneous hemodynamic fluctuations (e.g., BOLD, CBF, and CBV) may be attributed to the different species and brain states studied. In studies on anesthetized animals, both the depth of anesthesia and the type of anesthetic are likely to significantly affect spontaneous brain activity. On the one hand, this complexity may make it difficult to provide a generic understanding of spontaneous hemodynamic fluctuations and their neural origins. On the other hand, it also suggests that different brain states are associated with distinct spontaneous brain activities and thus different hemodynamic fluctuations, which can be readily imaged and investigated using noninvasive fMRI methods. This notion is supported by a series of recent studies, which observed spontaneous BOLD fluctuations and their organized spatial pattern (resting-brain coherent networks) across a wide range of resting-brain states from awake, sleep, lightly sedated, or even vegetative human brains (Biswal et al. 1995; Greicius et al. 2008; Horovitz et al. 2008; Boly et al. 2009) to lightly and deeply anesthetized primate brains (Vincent et al. 2007; Shmuel and Leopold 2008).

Spatial Characteristics of Coherent BOLD Fluctuations

The correlation maps based on the spatiotemporal correlation analysis of BOLD signals in the present study cover a large portion of the cortical regions in the scanned fMRI slices, and the relocation of the reference region within these cortical areas or changing the size of the reference region did not significantly change the spatial pattern of the correlation maps. Although the majority of these brain regions showing strong BOLD correlations still belong to the sensorimotor system, our results differ from those of previous studies investigating functional connectivity within the rat somatosensory system. In those studies, a more specific network mainly covering the bilateral S1FL regions was identified through spatiotemporal correlations of spontaneous CBV (or BOLD) fluctuation in rats

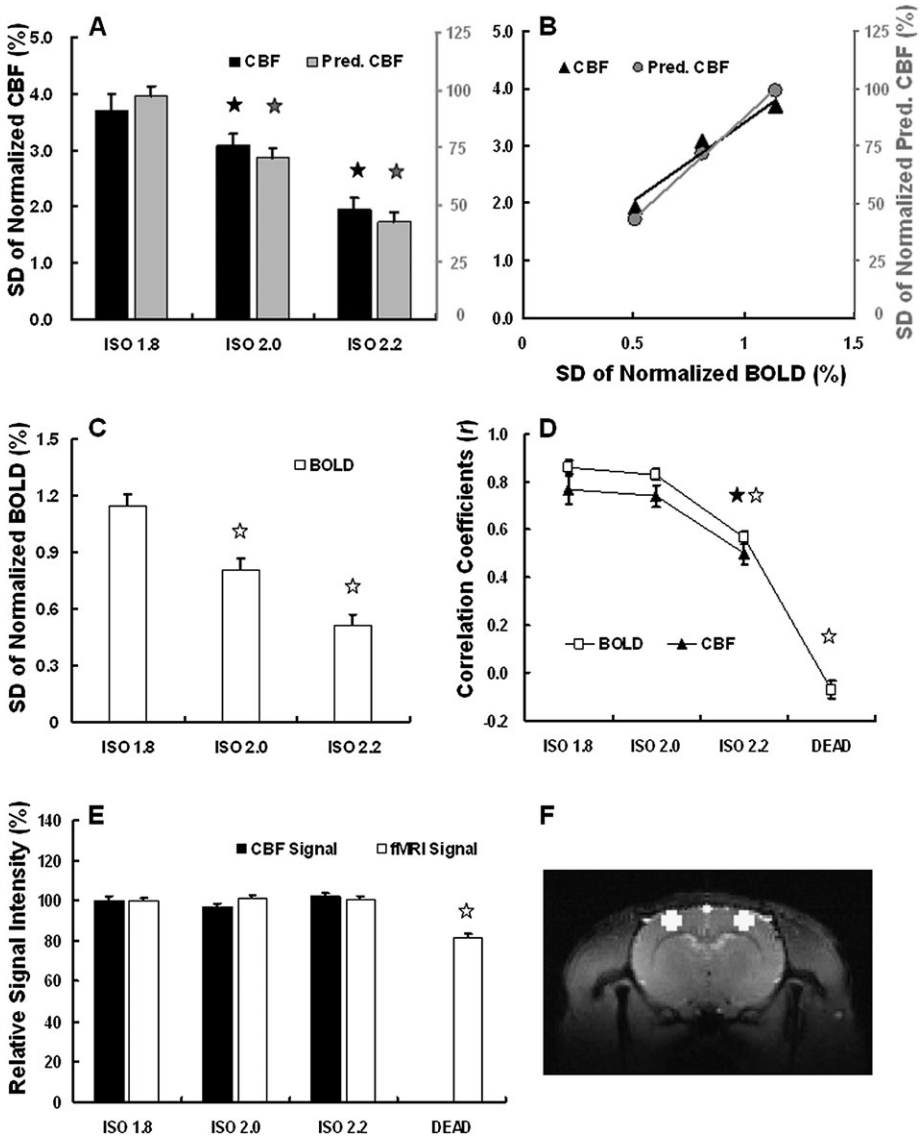

Figure 6. Multimodal comparisons and statistical summary of fluctuation magnitudes and coherence strength among the measured CBF, EEG-predicted CBF, and BOLD signals. The SDs of normalized CBF (*A*, black), EEG-predicted CBF (*A*, gray), and BOLD (*C*) signals, which quantify the fluctuation magnitudes, decrease as the anesthesia depth increases. Such dependences show an excellent linear correlation between CBF and BOLD signals ($R^2 = 0.96$, *B*, black triangles), as well as between EEG-predicted CBF and BOLD ($R^2 = 0.99$, *B*, gray circles). The interhemisphere correlations, which quantify the coherence strength of spontaneous fluctuations, also show the similar dependency on the anesthesia depth for the CBF and BOLD signals (*D*). The baseline levels of both CBF and fMRI signals did not change significantly under the 3 anesthesia conditions (*E*). An example of ROIs used for calculating BOLD statistics (see Materials and Methods) is shown with white color (*F*). The error bars in this figure represent the standard error of the mean. All comparisons were made with the ISO 1.8 anesthesia condition, and the pentacles are used to mark the conditions showing a statistically significant difference ($P < 0.01$).

anesthetized with α-chloralose (Lu et al. 2007) or medetomidine (Zhao et al. 2008). This discrepancy could again be due to the distinct spontaneous neural activities, as well as their different spatiotemporal correlations, induced by the different anesthetics and/or anesthesia depth.

As reported previously (Swank 1949; Steriade et al. 1994; Hudetz and Imas 2007), the burst–suppression activity is characterized by wide synchronization over the whole neocortex, although the strength of the bursts may not be uniform over all brain regions (Hudetz and Imas 2007). Furthermore, structural connectivity in the brain is essential for maintaining such synchronization since a lesion in the corpus callosum produced asymmetric (not coherent) burst–suppression patterns between 2 hemispheres (Lambrakis et al. 1999; Lazar et al. 1999). These electrophysiological studies are consistent with our observations based on the BOLD correlation maps, which reflect the large-scale synchronization of underlying neural activity and reveal the "functional connectivity" in the unconscious burst–suppression anesthesia condition.

According to a new theory about consciousness and anesthesia (Hudetz 2006; Alkire et al. 2008), loss of consciousness could be due to 2 mechanisms. One is the breakdown of cortical connectivity and thus of integration, and the other is the collapse of the repertoire of cortical activity pattern and thus of information even though the information may still be integrated globally. The strong but less-specific "connectivity" observed under burst–suppression anesthesia herein can be regarded as a valuable illustration of the second mechanism of the theory. It suggests that although the deeply anesthetized brain characterized by burst–suppression activity has already

completely lost consciousness, spontaneous neural activity could still be highly synchronized over different brain regions.

Even though the BOLD correlation is widely distributed and less-specific under the burst–suppression anesthesia, the correlation maps (e.g., Rat 3 in Fig. 4) show a trend that the strongest correlation with the right S1FL reference region usually appears at the contralateral S1FL region. This observation was further confirmed by either using a higher CC threshold for displaying the correlation maps or applying the global signal regression procedure (Fox et al. 2009) to removing the global correlations of BOLD signals, and the remaining fMRI pixels with strong coherence indeed located within the S1FL regions, bilaterally. This finding may suggest that the coherence of widely distributed and synchronized burst–suppression activity is still relatively stronger between the brain regions with the most intense anatomical connections. Therefore, the specificity of the BOLD coherent network reduced substantially under deeply anesthetized and unconscious brain state; however, it was not completely disappeared.

Our results also indicate a correlation between cortical regions and subcortical regions, including some thalamic nuclei and the CPu, although its correlation strength was relatively weaker than the corticocortical correlation. It is still not fully understood whether the thalamus and neocortex are functionally connected to each other under deep burst–suppression anesthesia. Earlier studies suggested that the neocortex is isolated from thalamic sensory inputs under burst–suppression anesthesia because the firing activity of cortical neurons is correlated with the EEG burst–suppression pattern but is independent of the thalamic neuron firing pattern (Steriade et al. 1994; Topolnik et al. 2003). Moreover, undercut anesthetized neocortex can still generate burst–suppression activity (Swank 1949; Topolnik et al. 2003). However, this view may need further investigation based on new evidence from a number of studies showing that a variety of sensory stimuli (visual, auditory, and somatosensory) were able to nonspecifically elicit global burst activity under burst–suppression anesthesia conditions (Hartikainen et al. 1995; Hudetz and Imas 2007; Kroeger and Amzica 2007). Our findings may provide some clues with regard to this issue and also suggest that the fMRI technique may provide a useful neuroimaging tool for future research on this topic.

Technical Considerations

Since the major focus of the present study was to investigate the neurovascular couplings underlying spontaneous BOLD fluctuations, it ideally required simultaneous EEG–BOLD measurement. However, this experimental configuration still faces many technical challenges; for example, to deal with the increased susceptibility effects that could lead to severe fMRI artifacts, especially at ultrahigh field. Therefore, 2 separate experiments were carefully designed and conducted in the present study to avoid these technical difficulties and complications. The rigorous multimodal comparisons and statistical analysis of the data obtained from these 2 experiments not only found very similar "bumps" in the BOLD and CBF signals but also indicated almost identical dependence of their fluctuations on anesthesia depth, leading to the conclusion that tight EEG–BOLD coupling exists in the isoflurane-anesthetized rat brain.

The HRF applied in the present study to link the EEG and CBF signals was taken from a previous study using a rat model and urethane anesthesia (Martin et al. 2006). From the results of crosscorrelation functions between the EEG-predicted CBF and measured CBF (Fig. 2), the applied HRF seems to work slightly better under the ISO 2.0 anesthesia condition than under the ISO 1.8 anesthesia condition, whose correlation function peak appeared slightly ahead of zero lag (Fig. 2*A*). This observation raises an interesting question: does the HRF alter under different anesthesia conditions? Nevertheless, our analyses indicated that the correlation between the EEG-predicted CBF and experimentally measured CBF was less sensitive to the precise shape of the HRF applied. For instance, the use of the HRF from awake human brain, which has a much longer BOLD peak latency and broad HRF shape compared with the rat brain HRF, did not significantly change the outcomes and conclusions. Moreover, the rat brain HRF taken from the literature was similar with the HRF deconvolved from the EEG-CBF data obtained in the present study. Therefore, it provided a good approximation for examining the EEG-CBF coupling relation.

The raw data of spontaneous CBF and fMRI time courses measured in the present study were both in arbitrary unit; thus, they were normalized by their mean signals before the SDs were calculated to quantify the CBF and BOLD fluctuation magnitudes. One potential complication is that a significant change in baseline perfusion level (CBF) or baseline fMRI signal under varied anesthesia conditions or in a dead brain may affect the reference level of normalization and thus quantification of fluctuation magnitude. To address this concern, the baseline levels of CBF and fMRI signals were examined and compared under all the conditions studied herein, and no significant difference was found between the 3 anesthesia conditions (Fig. 6*E*) except for a significant fMRI signal reduction in the dead rat brain due to a large decrease in the blood oxygenation level. This result is not surprising since the global perfusion level of rat brain increased by only ~10% when isoflurane was increased from 1.4% to 2.8%, as reported previously (Lenz et al. 1998). A much narrower range (1.8–2.2%) of isoflurane concentration was applied in the present study, and the anesthetic and vasodilatation effects of isoflurane may compensate each other within this range such that baseline CBF and fMRI levels did not change, as shown in Figure 6*E*. Therefore, the SD of normalized CBF/BOLD signals should provide a reliable quantitative indicator reflecting the magnitude of the hemodynamic fluctuation.

Other Perspectives

Recent research on neuroenergetics using neuroimaging techniques has revealed that a large portion of the total brain energy is used to support the spontaneous neural activity and "housekeeping" power in the brain (Raichle 2006; Raichle and Mintun 2006; Shulman et al. 2007; Du et al. 2008). Also interestingly, the prestimulus baseline hemodynamic signals have been found to be linked to human behavioral responses and can influence task-evoked brain activity (Sapir et al. 2005; Boly et al. 2007; Fox et al. 2007; Hesselmann et al. 2008). These findings emphasize the essential roles of spontaneous brain activity in supporting basic brain function and in understanding the working mechanism of the brain. The large hemodynamic fluctuations and their highly organized spatial coherence as observed under the unconscious brain state in the present study support these findings. Although the measured

spontaneous CBF and BOLD signal changes cannot be used to directly determine the absolute baseline energy levels in the rat brain, they indeed imply a high brain energy demand for supporting the large CBF/BOLD fluctuations, which showed similar magnitudes to those evoked by brain stimulation. Since relative CBF and BOLD changes can be quantitatively linked to the change in the cerebral metabolic rate of oxygen consumption ($CMRO_2$) by using the BOLD calibration model (Kim and Ugurbil 1997; Davis et al. 1998), the observed tight coupling between spontaneous CBF and BOLD signal changes in this study indirectly implies a substantial $CMRO_2$ or energy fluctuation for supporting spontaneous brain activity.

It has been documented that a loss of bilateral and symmetric burst–suppression EEG synchronization between 2 hemispheres is a clinical indication of brain dysfunction (e.g., unilateral brain infarction or stroke) (Stern and Engel 2005). The neuroimaging approaches based on either BOLD or CBF signal source should provide a sensitive tool for noninvasively imaging and diagnosing these types of brain dysfunction with superior spatial and temporal resolution.

Conclusion

Several conclusions can be drawn from the present study. There is tight neurovascular coupling between the spontaneous EEG amplitude and spontaneous hemodynamic (CBF and BOLD) fluctuations in the deeply anesthetized unconscious brain state characterized by burst–suppression EEG activity. The coupled EEG, CBF, and BOLD signals were highly synchronized in large-scale cortical regions as well as some of the subcortical nuclei associated with the sensorimotor system. The synchronization pattern of spontaneous brain activities can be mapped by fMRI based on spatiotemporal correlations of low-frequency BOLD fluctuations, resulting in "coherent networks" in the deeply anesthetized rat brain. It was also found that the coherence strength and fluctuation amplitude of spontaneous hemodynamic signals as well as the spatial extent of the mapped "coherent networks" are sensitive to the patterns of spontaneous brain activity, which can be modulated by anesthesia depth or other interventions. The overall findings support the conclusion that the spontaneous CBF/BOLD fluctuations observed under burst–suppression anesthesia conditions are mainly of neural origin. They provide valuable insights into the neurophysiological basis for the use of BOLD- and CBF-based fMRI methods to investigate spontaneous and synchronous brain activity under various brain states.

Supplementary Material

Supplementary material can be found at: http://www.cercor.oxfordjournals.org/.

Funding

National Institutes of Health (NS041262, NS041262S1, EB000329, NS057560, P41 RR008079, and P30NS057091); Keck Foundation.

Notes

The authors thank Dr Nanyin Zhang, Dr Fei Du, and Ms Xiao Wang for technical assistance and discussion, and Dr Kamil Ugurbil for support.
Conflict of Interest : None declared.

References

Alkire MT, Hudetz AG, Tononi G. 2008. Consciousness and anesthesia. Science. 322:876–880.

Bandettini PA, Wong EC, Hinks RS, Tikofsky RS, Hyde JS. 1992. Time course EPI of human brain function during task activation. Magn Reson Med. 25:390–397.

Biswal B, Hudetz AG, Yetkin FZ, Haughton VM, Hyde JS. 1997. Hypercapnia reversibly suppresses low-frequency fluctuations in the human motor cortex during rest using echo-planar MRI. J Cereb Blood Flow Metab. 17:301–308.

Biswal B, Yetkin FZ, Haughton VM, Hyde JS. 1995. Functional connectivity in the motor cortex of resting human brain using echo-planar MRI. Magn Reson Med. 34:537–541.

Boly M, Balteau E, Schnakers C, Degueldre C, Moonen G, Luxen A, Phillips C, Peigneux P, Maquet P, Laureys S. 2007. Baseline brain activity fluctuations predict somatosensory perception in humans. Proc Natl Acad Sci U S A. 104:12187–12192.

Boly M, Tshibanda L, Vanhaudenhuyse A, Noirhomme Q, Schnakers C, Ledoux D, Boveroux P, Garweg C, Lambermont B, Phillips C, et al. 2009. Functional connectivity in the default network during resting state is preserved in a vegetative but not in a brain dead patient. Hum Brain Mapp. 30:2393–2400.

Cordes D, Haughton VM, Arfanakis K, Wendt GJ, Turski PA, Moritz CH, Quigley MA, Meyerand ME. 2000. Mapping functionally related regions of brain with functional connectivity MR imaging. AJNR Am J Neuroradiol. 21:1636–1644.

Davis TL, Kwong KK, Weisskoff RM, Rosen BR. 1998. Calibrated functional MRI: mapping the dynamics of oxidative metabolism. Proc Natl Acad Sci U S A. 95:1834–1839.

Du F, Zhu XH, Zhang Y, Friedman M, Zhang N, Ugurbil K, Chen W. 2008. Tightly coupled brain activity and cerebral ATP metabolic rate. Proc Natl Acad Sci U S A. 105:6409–6414.

Fair DA, Cohen AL, Dosenbach NU, Church JA, Miezin FM, Barch DM, Raichle ME, Petersen SE, Schlaggar BL. 2008. The maturing architecture of the brain's default network. Proc Natl Acad Sci U S A. 105:4028–4032.

Feige B, Scheffler K, Esposito F, Di Salle F, Hennig J, Seifritz E. 2005. Cortical and subcortical correlates of electroencephalographic alpha rhythm modulation. J Neurophysiol. 93:2864–2872.

Fox MD, Raichle ME. 2007. Spontaneous fluctuations in brain activity observed with functional magnetic resonance imaging. Nat Rev Neurosci. 8:700–711.

Fox MD, Snyder AZ, Vincent JL, Raichle ME. 2007. Intrinsic fluctuations within cortical systems account for intertrial variability in human behavior. Neuron. 56:171–184.

Fox MD, Zhang D, Snyder AZ, Raichle ME. 2009. The global signal and observed anticorrelated resting state brain networks. J Neurophysiol. 101:3270–3283.

Golanov EV, Yamamoto S, Reis DJ. 1994. Spontaneous waves of cerebral blood flow associated with a pattern of electrocortical activity. Am J Physiol. 266:R204–R214.

Goldman RI, Stern JM, Engel J, Jr, Cohen MS. 2002. Simultaneous EEG and fMRI of the alpha rhythm. Neuroreport. 13:2487–2492.

Greicius MD, Kiviniemi V, Tervonen O, Vainionpaa V, Alahuhta S, Reiss AL, Menon V. 2008. Persistent default-mode network connectivity during light sedation. Hum Brain Mapp. 29:839–847.

Greicius MD, Krasnow B, Reiss AL, Menon V. 2003. Functional connectivity in the resting brain: a network analysis of the default mode hypothesis. Proc Natl Acad Sci U S A. 100:253–258.

Hampson M, Peterson BS, Skudlarski P, Gatenby JC, Gore JC. 2002. Detection of functional connectivity using temporal correlations in MR images. Hum Brain Mapp. 15:247–262.

Hartikainen KM, Rorarius M, Perakyla JJ, Laippala PJ, Jantti V. 1995. Cortical reactivity during isoflurane burst–suppression anesthesia. Anesth Analg. 81:1223–1228.

Hesselmann G, Kell CA, Eger E, Kleinschmidt A. 2008. Spontaneous local variations in ongoing neural activity bias perceptual decisions. Proc Natl Acad Sci U S A. 105:10984–10989.

Horovitz SG, Fukunaga M, de Zwart JA, van Gelderen P, Fulton SC, Balkin TJ, Duyn JH. 2008. Low frequency BOLD fluctuations during

resting wakefulness and light sleep: a simultaneous EEG-fMRI study. Hum Brain Mapp. 29:671–682.
Hudetz AG. 2006. Suppressing consciousness: mechanisms of general anesthesia. Seminars Anesth Periop Med Pain. 25:196–204.
Hudetz AG, Imas OA. 2007. Burst activation of the cerebral cortex by flash stimuli during isoflurane anesthesia in rats. Anesthesiology. 107:983–991.
Hudetz AG, Roman RJ, Harder DR. 1992. Spontaneous flow oscillations in the cerebral cortex during acute changes in mean arterial pressure. J Cereb Blood Flow Metab. 12:491–499.
Kannurpatti SS, Biswal BB, Kim YR, Rosen BR. 2008. Spatio-temporal characteristics of low-frequency BOLD signal fluctuations in isoflurane-anesthetized rat brain. Neuroimage. 40:1738–1747.
Kim SG, Ugurbil K. 1997. Comparison of blood oxygenation and cerebral blood flow effects in fMRI: estimation of relative oxygen consumption change. Magn Reson Med. 38:59–65.
Kroeger D, Amzica F. 2007. Hypersensitivity of the anesthesia-induced comatose brain. J Neurosci. 27:10597–10607.
Kwong KK, Belliveau JW, Chesler DA, Goldberg IE, Weisskoff RM, Poncelet BP, Kennedy DN, Hoppel BE, Cohen MS, Turner R, et al. 1992. Dynamic magnetic resonance imaging of human brain activity during primary sensory stimulation. Proc Natl Acad Sci U S A. 89:5675–5679.
Lambrakis CC, Lancman ME, Romano C. 1999. Asynchronous and asymmetric burst–suppression in a patient with a corpus callosum lesion. Clin Neurophysiol. 110:103–105.
Lazar LM, Milrod LM, Solomon GE, Labar DR. 1999. Asynchronous pentobarbital-induced burst suppression with corpus callosum hemorrhage. Clin Neurophysiol. 110:1036–1040.
Lenz C, Rebel A, van Ackern K, Kuschinsky W, Waschke KF. 1998. Local cerebral blood flow, local cerebral glucose utilization, and flow-metabolism coupling during sevoflurane versus isoflurane anesthesia in rats. Anesthesiology. 89:1480–1488.
Logothetis NK, Murayama Y, Augath M, Steffen T, Werner J, Oeltermann A. 2009. How not to study spontaneous activity. Neuroimage. 45:1080–1089.
Lowe MJ, Mock BJ, Sorenson JA. 1998. Functional connectivity in single and multislice echoplanar imaging using resting-state fluctuations. Neuroimage. 7:119–132.
Lu H, Zuo Y, Gu H, Waltz JA, Zhan W, Scholl CA, Rea W, Yang Y, Stein EA. 2007. Synchronized delta oscillations correlate with the resting-state functional MRI signal. Proc Natl Acad Sci U S A. 104:18265–18269.
Lund TE. 2001. fcMRI–mapping functional connectivity or correlating cardiac-induced noise? Magn Reson Med. 46:628–629.
Mansfield P. 1977. Multi-planar image formation using NMR spin-echos. J Phys C: Solid State Physics. 10:L55–L58.
Mantini D, Perrucci MG, Del Gratta C, Romani GL, Corbetta M. 2007. Electrophysiological signatures of resting state networks in the human brain. Proc Natl Acad Sci U S A. 104:13170–13175.
Martin C, Martindale J, Berwick J, Mayhew J. 2006. Investigating neural-hemodynamic coupling and the hemodynamic response function in the awake rat. Neuroimage. 32:33–48.
Moosmann M, Ritter P, Krastel I, Brink A, Thees S, Blankenburg F, Taskin B, Obrig H, Villringer A. 2003. Correlates of alpha rhythm in functional magnetic resonance imaging and near infrared spectroscopy. Neuroimage. 20:145–158.
Morcom AM, Fletcher PC. 2007. Does the brain have a baseline? Why we should be resisting a rest. Neuroimage. 37:1073–1082.
Ogawa S, Lee T-M, Kay AR, Tank DW. 1990. Brain magnetic resonance imaging with contrast dependent on blood oxygenation. Proc Natl Acad Sci U S A. 87:9868–9872.
Ogawa S, Menon RS, Kim S-G, Ugurbil K. 1998. On the characteristics of functional magnetic resonance imaging of the brain. Annu Rev Biophys Biomol Struct. 27:447–474.
Ogawa S, Tank DW, Menon R, Ellermann JM, Kim SG, Merkle H, Ugurbil K. 1992. Intrinsic signal changes accompanying sensory stimulation: functional brain mapping with magnetic resonance imaging. Proc Natl Acad Sci U S A. 89:5951–5955.
Paxinos G, Watson C. 1998. The rat brain in stereotaxic coordinates. San Diego (CA): Academic Press.
Pinheiro J, Bates D, DebRoy S, Sarkar D. The R Core team. 2009. nlme: Linear and Nonlinear Mixed Effects Models. R package version 3. 1–93.
R Development Core Team (2008). R: A language and environment for statistical computing. Vienna (Austria): R Foundation for Statistical Computing, Available at http://www.R-project.org.
Raichle ME. 2006. Neuroscience. The brain's dark energy. Science. 314:1249–1250.
Raichle ME, Mintun MA. 2006. Brain work and brain imaging. Annu Rev Neurosci. 29:449–476.
Sapir A, d'Avossa G, McAvoy M, Shulman GL, Corbetta M. 2005. Brain signals for spatial attention predict performance in a motion discrimination task. Proc Natl Acad Sci U S A. 102:17810–17815.
Shmuel A, Leopold DA. 2008. Neuronal correlates of spontaneous fluctuations in fMRI signals in monkey visual cortex: implications for functional connectivity at rest. Hum Brain Mapp. 29:751–761.
Shulman RG, Rothman DL, Hyder F. 2007. A BOLD search for baseline. Neuroimage. 36:277–281.
Stein T, Moritz C, Quigley M, Cordes D, Haughton V, Meyerand E. 2000. Functional connectivity in the thalamus and hippocampus studied with functional MR imaging. AJNR Am J Neuroradiol. 21:1397–1401.
Steriade M, Amzica F, Contreras D. 1994. Cortical and thalamic cellular correlates of electroencephalographic burst–suppression. Electroencephalogr Clin Neurophysiol. 90:1–16.
Stern JM, Engel J. 2005. Atlas of EEG patterns. Philadelphia (PA): Lippincott Williams & Wilkins. p. 107–108.
Swank RL. 1949. Synchronization of spontaneous electrical activity of cerebrum by barbiturate narcosis. J Neurophysiol. 12:161–172.
Topolnik L, Steriade M, Timofeev I. 2003. Partial cortical deafferentation promotes development of paroxysmal activity. Cereb Cortex. 13:883–893.
Vincent JL, Patel GH, Fox MD, Snyder AZ, Baker JT, Van Essen DC, Zempel JM, Snyder LH, Corbetta M, Raichle ME. 2007. Intrinsic functional architecture in the anaesthetized monkey brain. Nature. 447:83–86.
Zhao F, Zhao T, Zhou L, Wu Q, Hu X. 2008. BOLD study of stimulation-induced neural activity and resting-state connectivity in medetomidine-sedated rat. Neuroimage. 39:248–260.